

RESEARCH ARTICLE

Evaluation of the anatomical variations of the coronary venous system in patients with coronary artery calcification using 256-slice computed tomography

Wei Bai^{1,2}, Xiao Xu¹, Haixia Ji¹, Jing Liu^{1*}, Heng Ma^{1,3*}, Haizhu Xie^{1,3}, Jianjun Dong¹, Chunjuan Sun¹, Yinghong Shi¹, Kaili Che¹, Meijie Liu³, Yingkun Guo^{2*}

1 Yantai Yuhuangding Hospital, Qingdao University, Yantai, Shandong Province, China, **2** Department of Radiology, Key Laboratory of Obstetric & Gynecologic and Pediatric Diseases and Birth Defects of Ministry of Education, West China Second University Hospital, Sichuan University, Chengdu, Sichuan Province, China, **3** Binzhou Medical University, Yantai, Shandong Province, China

☯ These authors contributed equally to this work.

* liujingyhd@126.com (JL); hengma00@163.com (HM); gykpanda@163.com (YG)



OPEN ACCESS

Citation: Bai W, Xu X, Ji H, Liu J, Ma H, Xie H, et al. (2020) Evaluation of the anatomical variations of the coronary venous system in patients with coronary artery calcification using 256-slice computed tomography. PLoS ONE 15(11): e0242216. <https://doi.org/10.1371/journal.pone.0242216>

Editor: Alexander H. Maass, University Medical Center Groningen, University of Groningen, NETHERLANDS

Received: July 4, 2020

Accepted: October 28, 2020

Published: November 18, 2020

Copyright: © 2020 Bai et al. This is an open access article distributed under the terms of the [Creative Commons Attribution License](https://creativecommons.org/licenses/by/4.0/), which permits unrestricted use, distribution, and reproduction in any medium, provided the original author and source are credited.

Data Availability Statement: All relevant data are within the paper.

Funding: This work was funded by National Natural Science Foundation of China No.81671654, awarded to H.M., H.X, C.J., Y.H. The funders had no role in study design, data collection and analysis, decision to publish, or preparation of the manuscript.

Abstract

The factors that determine the anatomical variations of the coronary venous system (CVS) are poorly understood. The objective of this study was to evaluate the anatomical variations of the CVS in patients with coronary artery calcification. 196 patients underwent non-contrast CT and coronary CT angiography using 256-slice CT. All subjects were divided into four groups based on their coronary artery calcium score (CACS): 50 patients with CACS = 0 Agatston unit (AU), 52 patients with CACS = 1–100 AU, 44 patients with CACS = 101–400 AU, and 50 patients with CACS > 400 AU. The presence of the following cardiac veins was evaluated: the coronary sinus (CS), great cardiac vein (GCV), posterior interventricular vein (PIV), posterior vein of the left ventricle (PVLV), left marginal vein (LMV), anterior interventricular vein (AIV), and small cardiac vein (SCV). Vessel diameters were also measured. We found that the CS, GCV, PIV, and AIV were visualized in all patients, whereas the PVLV and LMV were identified in a certain proportion of patients: 98% and 96% in the CACS = 0 AU group, 100% and 78.8% in the CACS = 1–100 AU group, 93.2% and 77.3% in the CACS = 101–400 AU group, and 98% and 78% in the CACS > 400 AU group, respectively. The LMV was less often identified in the last three groups than in the first group ($p < 0.05$). The frequency of having either one PVLV or LMV was higher in the last three groups than in the first group ($p < 0.05$). No significant differences in vessel diameters were observed between the groups. It was concluded that patients with coronary artery calcification were less likely to have the LMV, which might hamper the left ventricular lead implantation in cardiac resynchronization therapy.

Competing interests: The authors have declared that no competing interests exist.

Introduction

Over the past decade, our knowledge of the coronary venous system (CVS) has increased because of advances in interventional cardiac procedures, such as cardiac resynchronization therapy (CRT), percutaneous mitral annuloplasty, and radiofrequency catheter ablation [1–4]. The anatomical variations of the CVS have become one of the most investigated issues, because a knowledge of the CVS anatomy is necessary and significant before interventional processes within CVS, which can increase the success rate of the operations [5]. However, the factors that determine the anatomical variations of the CVS are poorly understood.

The anatomy of the CVS in patients with myocardial infarction (MI) or heart failure varies [6, 7]. Van de Veire et al. [7] studied 100 subjects via 64-slice computed tomography (CT) and found that the frequency of having no left marginal veins (LMV) was higher in patients with previous MI than in patients without MI. MI occurs when the blood flow to the heart is decreased or completely blocked. The complete blockage of the coronary artery is often caused by the rupture of an atherosclerotic plaque which is usually the underlying mechanism of a MI. Coronary artery calcification is an important coronary atherosclerosis sign, which is closely related to the severity of coronary atherosclerosis [8]. In an interesting study, Mlynarska et al. [9] used a 64-slice CT scan to assess the relationship between variation in the coronary veins and the extent of coronary artery calcium score (CACS) that can reflect the severity of coronary atherosclerosis. They found the subjects with higher CACS (> 100 AU) had more visible coronary veins (≥ 5) than the groups with lower and no CACS. However, they didn't analyze the specific variation in each vein. To our best knowledge, studies about the effect of coronary artery calcification on the anatomy of the CVS by using 256-slice CT have not been conducted. Therefore, our study aimed to assess the anatomical variations of the CVS in patients with coronary artery calcification in detail by using 256-slice CT.

Materials and methods

Study population

The anatomy of the CVS and CACS were retrospectively studied in 196 consecutive patients (96 females and 100 males; mean age: 63.3 ± 9.9 years). All patients underwent non-contrast CT and coronary CT angiography (CTA) between June 2018 and September 2019 for suspected coronary artery disease (CAD). These patients were divided into four groups based on the CACS: 50 (25.5%) patients without calcification (CACS = 0 AU, Agatston unit), 52 (26.5%) patients with minimal to mild calcification (CACS = 1–100 AU), 44 (22.4%) patients with moderate calcification (CACS = 101–400 AU), and 50 (25.5%) patients with severe calcification (CACS > 400 AU).

Patients with the following medical conditions were excluded from our study: atrial fibrillation, second- or third-degree atrioventricular block, renal insufficiency, creatinine level above 2 mg/dL, known allergy to iodine-containing contrast agents, and pregnancy. The study protocol was approved by the ethics committee of Yantai Yuhuangding Hospital. And the need for written informed patient consent was waived, because this was a retrospective study of coronary CT angiography performed for clinical purposes.

Coronary CT angiography protocol

Non-contrast CT and coronary CTA were conducted on the same day by using 256-slice CT (Brilliance iCT, Phillips, Cleveland, Ohio, USA). On the examination day, the patients were evaluated by measuring their heart rate and blood pressure 1 h prior to CT acquisition. An intravenous β -blocker was given to decrease patients' heart rate if it was higher than 90 bpm.

A low-dose non-contrast CT scan was performed to assess the CACS. Then, the coronary CTA was performed with the following scan parameters: tube voltage, 100 kVp; effective tube current time product, 700 mAs; pitch, 0.18; detector configuration, 128×0.625 mm; and rotation time, 270 ms. An average of 75 ml of contrast agent (Ultravist 370, Bayer Schering Pharma AG, Berlin, Germany) was injected in the antecubital vein at a rate of 5 ml/s by using a dual-head injector. First, 60 ml of contrast agent (average) was administered. Then 30 ml of a 1:1 mixture of contrast and saline was given; Lastly, 30 ml of saline was given. Retrospective electrocardiogram triggering was conducted to scan 45% and 75% of the RR interval. Automatic bolus tracking (Bolus Pro, Philips Healthcare, Cleveland, OH, USA) was performed in the ascending aorta, and coronary CTA scanning was automatically started 6 s after the predetermined threshold level of 180 Hounsfield units (HU) was reached.

Image reconstruction and analysis

The collected images were transferred to two designated workstations (IntelliSpace Portal, Cleveland, Ohio, USA; GE, Advantage Workstation, version 4.6) and analyzed. The CACS was assessed by using images with 2.5 mm slice thickness from non-contrast CT (Fig 1). In this procedure, pixels exceeding 130 HU were identified and encircled in the course of a coronary artery and calculated with the Agatston method [10]. For the anatomic observation of CVS, the following cardiac veins were evaluated on the collected images from the coronary CTA: the coronary sinus (CS), great cardiac vein (GCV), posterior interventricular vein (PIV), posterior vein of the left ventricle (PVLV), left marginal vein (LMV), anterior interventricular vein (AIV), and small cardiac vein (SCV) (Fig 2). Multiplanar reformatting was conducted to determine the size of the ostium of the CS in the anteroposterior and superoinferior direction. The proximal diameter of the GCV and the starting diameters of the PIV, PVLV, LMV and AIV were measured.

Statistical analysis

Continuous variables were expressed as mean \pm standard deviation. Differences between the groups were examined in terms of continuous variables via ANOVA. Categorical variables were expressed as absolute numbers (percentage) and analyzed with a χ^2 test. Data with P value < 0.05 were considered statistically significant. Statistical analyses were performed by using SPSS version 23.0.

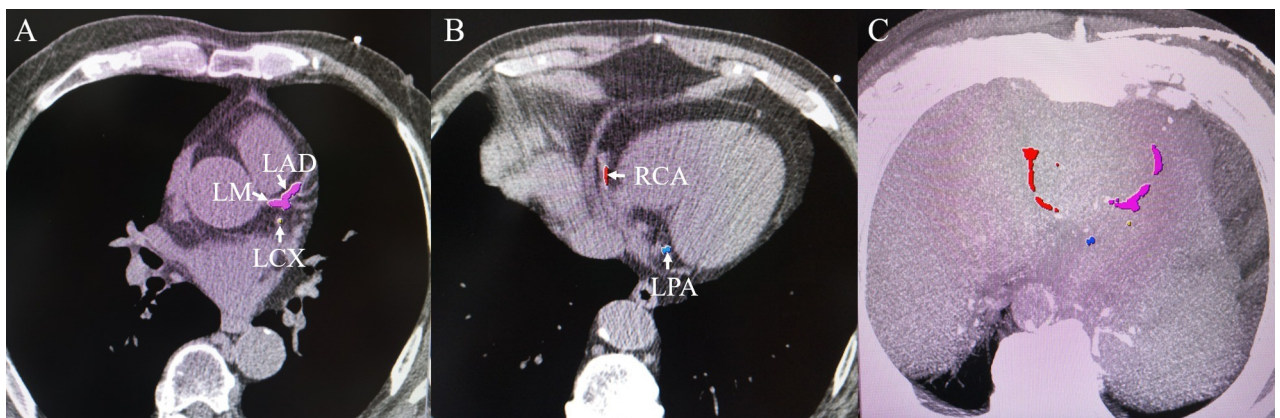


Fig 1. Example of the assessment of the coronary artery calcium score on axial images from the non-contrast CT. (A) and (B) Axial images; (C) superimposed axial images. Extensive calcification observed in the left main coronary artery (LM, pink), left anterior descending artery (LAD, pink), left circumflex coronary artery (LCX, yellow), right coronary artery (RCA, red), and posterior branch of the left ventricle artery (LPA, blue).

<https://doi.org/10.1371/journal.pone.0242216.g001>

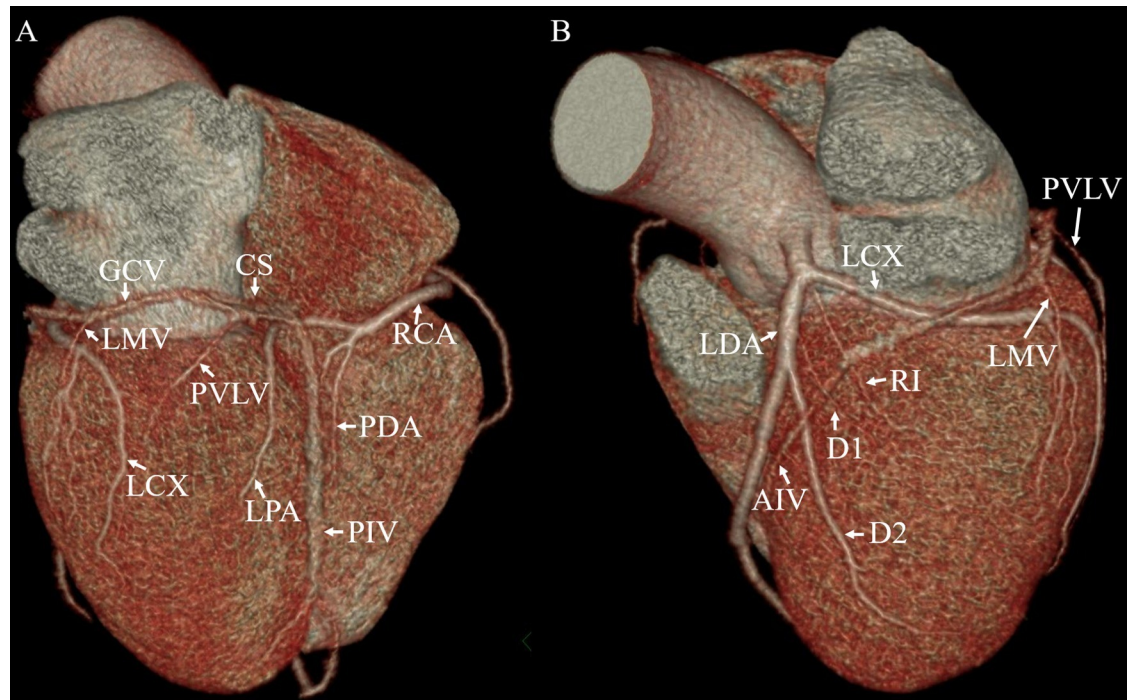


Fig 2. Volume-rendering image provides an overview of the evaluated coronary veins. (A) Posterior view; (B) anterolateral view. The coronary sinus (CS) and great cardiac vein (GCV) run along the atrioventricular groove. The posterior interventricular vein (PIV) is the first tributary of the CS that courses in the posterior interventricular groove. The other tributaries of the CS are the posterior vein of the left ventricle (PVLV) and the left marginal vein (LMV). The great cardiac vein (GCV) then continues as the anterior interventricular vein (AIV) in the anterior interventricular groove. Also note the left anterior descending artery (LAD), left circumflex coronary artery (LCX), ramus intermedius (RI), diagonal branches (D1, D2), posterior descending artery (PDA), posterior branch of left ventricle artery (LPA) and right coronary artery (RCA).

<https://doi.org/10.1371/journal.pone.0242216.g002>

Results

Baseline characteristics

The baseline characteristics of the patients included in this study are presented in [Table 1](#). The patients with coronary artery calcification in the last three groups were older than those who had no detectable CACS in the first group and the hemodynamic parameters, including EDV, ESV, and cardiac output of the former were higher than those of the latter. The frequency of cardiac risk factors, including smoking, diabetes, hypertension, and hypercholesterolemia was also higher in the former than in the latter. The CACS > 400 AU group of patients who had higher CACS was mostly composed of men.

Visualization of the coronary veins and CACS

The CS, GCV, PIV and AIV were visualized in all the patients (100%). [Table 2](#) shows the visualization of the PVLV and LMV in the four groups. Statistical differences were observed in cases without LMV visualized. The LMV was less often identified in the last three groups (CACS \geq 1 AU) than in the CACS = 0 AU group (Pearson Chi-squared = 8.381; $p = 0.039$). No statistical differences were observed in the visualization of the PVLV. The frequency of having either one PVLV or LMV and either PVLV or LMV (\geq 1) were higher in the last three groups than in the CACS = 0 AU group (Pearson Chi-squared = 8.430 and 9.208; $p = 0.038$ and 0.027). The percentages of SCV ($P > 0.05$) observed varied between groups: 7 (14.0%) subjects in the CACS = 0 AU group, 2 (3.8%) subjects in the CACS = 1–100 AU group, 7 (15.9%)

Table 1. Baseline characteristics of the study population.

CASS	0 AU (n = 50)	1–100 AU (n = 52)	101–400 AU (n = 44)	> 400 AU (n = 50)	P
Age, years	55.7 ± 8.7	63.7 ± 9.8	66.8 ± 8.4	67.4 ± 8.3	<0.01
Male, %	50	36.5	47.7	70	0.08
Hemodynamic parameters					
Ejection fraction, %	65.6 ± 9.9	66.9 ± 3.3	65.7 ± 5.4	66.1 ± 5.2	0.756
EDV, ml	122.5 ± 31.7	133.9 ± 37.8	135.5 ± 42.0	149.2 ± 45.9	0.021
ESV, ml	80.3 ± 18.1	90.0 ± 26.2	90.4 ± 26.2	98.2 ± 28.6	0.013
Cardiac output, L/min	5.9 ± 1.7	6.4 ± 2.0	6.0 ± 1.9	7.1 ± 2.2	0.016
Cardiovascular risk factors					
Heart Rate, bpm	77.8 ± 10.6	75.3 ± 10.9	74.2 ± 10.9	76.5 ± 11.0	0.449
Smoking, %	17.9	20.4	25.6	43.8	0.024
Diabetes, %	12.5	14.3	29.5	41.7	0.003
Hypertension, %	40.0	53.1	61.4	68.8	0.046
Hypercholesterolemia, %	32.5	53.2	27.9	31.1	0.049

EDV = left ventricular end-diastolic volume; ESV = left ventricular end-systolic volume.

<https://doi.org/10.1371/journal.pone.0242216.t001>

subjects in the CACS = 101–400 AU group and 5 (10%) subjects in the CACS > 400 AU group.

Quantitative measurement and CACS

The diameters of the CS ostium and its tributaries are presented in Table 3. The mean diameter of the CS ostium in the anteroposterior direction in all the patients was smaller than that in the superoinferior direction. No significant differences regarding the diameters of the CS ostium and its tributaries were noted in these groups.

Discussion

This study was the first to evaluate the relationship between the CVS and coronary artery calcification by using 256-slice CT. The incidence of LMV in patients with coronary artery calcification was lower than in patients without coronary artery calcification. The frequency of having either one PVLV or LMV in the patients with coronary artery calcification was higher than that of the patients without calcification. The decreased prevalence of the CS tributaries might hamper the access of patients who are considered for CRT to optimal left ventricle (LV) lead positioning. Before CRT implantation, the detailed images of the coronary vein anatomy

Table 2. Visualization of the PVLV and LMV.

CASS	0 AU (n = 50)	1–100 AU (n = 52)	101–400 AU (n = 44)	> 400 AU (n = 50)	p
PVLV	49 (98%)	52 (100%)	41 (93.2%)	49 (98%)	0.195
1 PVLV	36 (72%)	39 (75%)	26 (59.1%)	34 (68%)	0.373
2 or 3 PVLVs	13 (26%)	13 (25%)	15 (34.1%)	15 (30%)	0.754
LMV	48 (96%)	41 (78.8%)	34 (77.3%)	39 (78%)	0.039
1 LMV	42 (84%)	38 (73.1%)	30 (68.2%)	35 (70%)	0.283
2 or 3 LMVs	6 (12%)	3 (5.8%)	4 (9.1%)	4 (8%)	0.731
Either one PVLV or LMV	1 (2%)	9 (17.3%)	8 (18.2%)	10 (20%)	0.038
Either PVLV or LMV (≥1)	3(6%)	11(21.2%)	13(29.5%)	12(24%)	0.027

<https://doi.org/10.1371/journal.pone.0242216.t002>

Table 3. Diameters of the CS ostium and its tributaries (mm).

CASS	0 AU (n = 50)	1–100 AU (n = 52)	101–400 AU (n = 44)	> 400 AU (n = 50)	p
CSO anteroposterior	9.1 ± 2.6	8.9 ± 2.1	9.2 ± 2.6	9.6 ± 2.4	NS
CSO superoinferior	12.6 ± 2.3	12.0 ± 2.1	11.8 ± 3.0	12.6 ± 2.3	NS
GCV proximal	9.1 ± 2.2	9.0 ± 1.9	9.3 ± 2.3	9.4 ± 2.0	NS
PIV	5.3 ± 1.4	5.4 ± 1.2	5.3 ± 1.1	5.6 ± 1.4	NS
PVLV	3.0 ± 1.2	3.2 ± 1.2	3.2 ± 1.1	3.1 ± 1.1	NS
LMV	2.4 ± 0.9	2.3 ± 0.5	2.3 ± 0.8	2.4 ± 0.7	NS
AIV	3.8 ± 0.8	4.0 ± 0.9	3.9 ± 0.8	4.2 ± 1.0	NS

<https://doi.org/10.1371/journal.pone.0242216.t003>

in the target area could be obtained by using 256-slice CT and sequentially provide guidance for patients who are planned for the operation.

In the era of percutaneous interventional therapies for cardiac diseases, the high variability of coronary venous anatomy is a clinical focus and real challenge [11]. The presence, number, and course of the CS, GCV, PIV, and AIV are constant. By contrast, the presence, number, and course of the PVLV, LMV, and SCV are highly heterogeneous. The CS ostium is the primary point of entry into the coronary venous network. In our study, the size of the CS ostium in the anteroposterior direction was smaller than that in the superoinferior direction in all the patients, indicating that the ostium was oval. This finding was similar to those of Ma et al. [12] and Sun et al. [5]. The diameters of the CS ostium and its tributaries of many patients suffering from chronic systolic heart failure or receiving coronary bypass grafts (CABG) have significantly enlarged [13–16]. This condition may be a consequence of the increased coronary venous blood flow and increased right atrial pressure in patients with heart failure. The increased coronary venous blood flow is related to the severity of heart failure [17, 18]. Mlynarski et al. [16] revealed that the distribution of pressures within the arterial and venous vessels of patients who receive CABG changed after the operation. A high pressure in the CVS can cause the expansion of veins as a compensation mechanism. Nevertheless, Van de Veire et al. [7] found that the diameters of the CS ostium and its tributaries do not change in patients with a history of MI compared with patients who have significant CAD without a history of MI and patients who have normal coronary arteries. In the present study, no significant differences in the diameters of the CS ostium and its tributaries were noted among the four groups. This result might suggest that the size of the CS ostium and its tributaries was not correlated with coronary artery calcification.

The highest variability is observed in the number of tributaries between the PIV and AIV [5, 19–23]. Those tributaries mainly include PVLV and LMV. The prevalence of the PVLV and LMV varies in different studies when using various types of CT (Table 4). The PVLV and LMV are crucial for CRT because they are frequently used in the LV lead implantation.

Table 4. Prevalence of the PVLV and LMV obtained from different studies that evaluated the coronary venous system using various kinds of CT.

	Mao et al. [19]	Tada et al. [20]	Abbara et al. [21]	Mlynarski et al. [22]	Genc et al. [23]	Sun et al. [5]
Imaging technique	EBCT	8-slice CT	16-slice CT	64-slice CT	128-slice CT	256-slice CT
Study population	231	70*	54	199	357§	102
PVLV, %	81	94	79.6	62.3	87	77.5
LMV, %	78	84	92.6	80.4	87.9	66.7

*6 patients were not evaluated because of the poor image quality; §18 patients were not evaluated because of the poor image quality.

<https://doi.org/10.1371/journal.pone.0242216.t004>

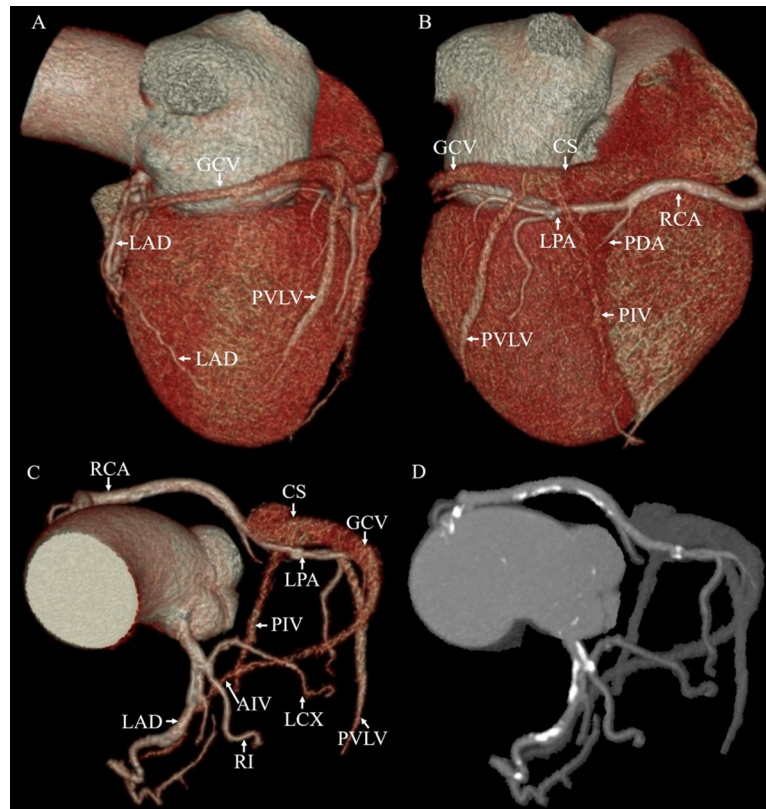


Fig 3. Volume-rendering images show absence of the left marginal vein (LMV) in a patient with CACS = 1201 AU. (A) Left lateral view of the heart; (B) posterior view of the heart; and (C) and (D) anterior views of the coronary tree. (D) shows the extensive calcification on the coronary artery. The coronary sinus (CS), great cardiac vein (GCV), posterior interventricular vein (PIV), posterior vein of the left ventricle (PVLV) and anterior interventricular vein (AIV) are visualized in this patient. Also note the left anterior descending artery (LAD), left circumflex coronary artery (LCX), ramus intermedius (RI), posterior descending artery (PDA), posterior branch of left ventricle artery (LPA) and right coronary artery (RCA).

<https://doi.org/10.1371/journal.pone.0242216.g003>

Evaluation of the coronary veins anatomy near the target region for potential LV lead implantation should be done to improve the success rate of CRT [24]. A recent study showed that the PVLV and LMV are less frequently present in CABG patients with reduced LV ejection fraction as compared to CABG patients with preserved LV ejection fraction, controls, and even non-ischemic cardiomyopathy [25]. Van de Veire et al. [7] who studied 100 subjects by using 64-slice CT and found the frequency of having no LMV was higher in patients with previous MI. These observations might indicate that the absence of LV tributaries in CAD patients with reduced LV ejection fraction or patients with a history of MI might preclude the transvenous placement of a LV lead and affect their CRT response. Our results were similar to those of Van de Veire et al [7]. We observed that the incidence of the LMV of the patients with coronary artery calcification was lower than that of the patients who had no calcification. ANOVA indicated no statistically significant differences in the prevalence of the LMV among the calcification groups. Fig 3 presents an example of an absent LMV in a patient with extensive coronary artery calcification. However, no statistically significant difference in the presence or absence of the PVLV was observed in the four groups in our study. Our findings might suggest that the coronary venous anatomy varied before MI happens. In this work, we also found that patients with coronary artery calcification had higher chance of having either one PVLV or LMV than

patients without calcification. It also indicated that patients with coronary artery calcification had fewer visible coronary veins. This result was inconsistent with the findings of Mlynarska et al. [9], which may be due to the use of different detection equipment or the insufficient sample size. This is a controversial issue that needs further study. We observed that the total number of the PVLV and LMV ranged from 1 to 5 and only three patients had 5 branches. Randhawa et al. [26] examined 50 formalin fixed adult cadaveric hearts and found that the total number of the PVLV and LMV ranges from 1 to 4. to some extent, their findings were consistent with ours. Furthermore, the number of optimal tributaries draining the lateral LV wall should be determined because the fewer the number of tributaries is, the less the scope of the optimal site selection of LV lead implantation will be [27].

Some limitations were identified in our study. First, the 256-slice CT scans were tailored for the optimal visualization of coronary arteries. Thus, no special scan and contrast protocol for venous enhancement were used, and the coronary veins with small diameters could not be visualized. Second, the relationship between the calcification of each coronary artery and the anatomical variations of adjacent coronary veins was not specifically analyzed in the present study, which is what we will do in the future studies. Other limitation was that multislice CT involves the use of a particular radiation dose and a contrast medium. Their required amounts can be decreased by applying the radiation- and contrast-sparing protocol of CTA on 256-slice CT [28].

Conclusion

The coronary venous anatomy varies in patients with coronary artery calcification. The LMV that constitutes one of the typical target veins for CRT may be less frequently present in patients with coronary artery calcification than in patients without coronary artery calcification, possibly making LV lead implantation more difficult during CRT. The pathophysiological mechanism of this finding should be further studied.

Acknowledgments

We would like to thank the staff of the Departments of Radiology in Yuhuangding Hospital for their help in our experiment.

Author Contributions

Conceptualization: Wei Bai, Xiao Xu, Jing Liu, Heng Ma, Haizhu Xie, Yingkun Guo.

Data curation: Wei Bai, Xiao Xu, Haixia Ji, Jing Liu, Heng Ma, Kaili Che, Meijie Liu.

Formal analysis: Wei Bai, Xiao Xu, Haixia Ji, Jing Liu, Heng Ma, Chunjuan Sun, Yinghong Shi, Yingkun Guo.

Funding acquisition: Heng Ma, Haizhu Xie, Chunjuan Sun, Yinghong Shi.

Investigation: Wei Bai, Xiao Xu, Haixia Ji, Heng Ma, Kaili Che, Meijie Liu.

Methodology: Wei Bai, Xiao Xu, Haixia Ji, Jing Liu, Heng Ma, Haizhu Xie, Chunjuan Sun, Yingkun Guo.

Project administration: Wei Bai, Xiao Xu, Haixia Ji, Jing Liu, Heng Ma, Haizhu Xie, Jianjun Dong, Yinghong Shi, Yingkun Guo.

Resources: Wei Bai, Xiao Xu, Jing Liu, Heng Ma, Haizhu Xie, Jianjun Dong, Yingkun Guo.

Software: Wei Bai, Xiao Xu, Heng Ma, Chunjuan Sun.

Supervision: Wei Bai, Xiao Xu, Jing Liu, Heng Ma, Haizhu Xie, Jianjun Dong, Yingkun Guo.

Validation: Wei Bai, Xiao Xu, Haixia Ji, Heng Ma, Chunjuan Sun, Kaili Che, Meijie Liu, Yingkun Guo.

Visualization: Wei Bai, Jing Liu, Heng Ma, Kaili Che, Meijie Liu, Yingkun Guo.

Writing – original draft: Wei Bai, Xiao Xu, Haixia Ji, Yingkun Guo.

Writing – review & editing: Wei Bai, Xiao Xu, Jing Liu, Heng Ma, Haizhu Xie, Jianjun Dong, Chunjuan Sun, Yinghong Shi.

References

1. Roka A, Borgquist R, Singh J. Coronary Sinus Lead Positioning. *Heart Failure Clin.* 2017; 13:79–91. <https://doi.org/10.1016/j.hfc.2016.07.007> PMID: 27886934
2. Giraldi F, Cattadori G, Roberto M, Corrado C, Mauro P, Giovanni B, et al. Long-term effectiveness of cardiac resynchronization therapy in heart failure patients with unfavorable cardiac veins anatomy comparison of surgical versus hemodynamic procedure. *J Am Coll Cardiol.* 2011; 58:483–490. <https://doi.org/10.1016/j.jacc.2011.02.065> PMID: 21777745
3. Baman TS, Ilg KJ, Gupta SK, Good E, Chugh A, Jongnarangsin K, et al. Mapping and ablation of epicardial idiopathic ventricular arrhythmias from within the coronary venous system. *Circ Arrhythm Electrophysiol.* 2010; 3:274–279. <https://doi.org/10.1161/CIRCEP.109.910802> PMID: 20400776
4. Mlynarski R, Mlynarska A, Sosnowski M. Coronary venous system in cardiac computer tomography: Visualization, classification and role. *World J Radiol.* 2014; 28:6:399–408. <https://doi.org/10.4329/wjr.v6.i7.399> PMID: 25071880
5. Sun C, Pan Y, Wang H, Li J, Nie P, Wang X, et al. Assessment of the coronary venous system using 256-slice computed tomography. *PLoS One.* 2014; 9:e104246. <https://doi.org/10.1371/journal.pone.0104246> PMID: 25089900
6. Ma H, Wang X, Xie H, Sun C, Wen Z, Liu Y, et al. Characterization of the cardiac venous system in heart failure patients using 256-slice CT. *Int J Cardiol.* 2016; 203:447–448. <https://doi.org/10.1016/j.ijcard.2015.10.135> PMID: 26547051
7. Van de Veire NR, Schuijff JD, De Sutter J, Devos D, Bleeker GB, de Roos A, et al. Non-invasive visualization of the cardiac venous system in CAD patients using 64-slice computed tomography. *J Am Coll Cardiol.* 2006; 48:1832–1838. <https://doi.org/10.1016/j.jacc.2006.07.042> PMID: 17084258
8. Shao JS, Cai J, Towler DA. Molecular mechanisms of vascular calcification: lessons learned from the aorta. *Arterioscler Thromb Vasc Biol.* 2006; 26:1423–1430. <https://doi.org/10.1161/01.ATV.0000220441.42041.20> PMID: 16601233
9. Mlynarska A, Mlynarski R, Sosnowski M. Variation in Cardiac Vein System is Associated with Coronary Artery Calcium—A Venous-Atherosclerosis Paradox? *Acta Cardiol Sin.* 2015; 31:536–542. <https://doi.org/10.6515/acs20150204b> PMID: 27122919
10. Agatston AS, Janowitz WR, Hildner FJ, Zusmer NR, Viamonte M Jr, Detrano R. Quantification of coronary artery calcium using ultrafast computed tomography. *J Am Coll Cardiol.* 1990; 15:827–32. [https://doi.org/10.1016/0735-1097\(90\)90282-t](https://doi.org/10.1016/0735-1097(90)90282-t) PMID: 2407762
11. Christiaens L, Ardilouze P, Ragot S, Mergy J, Allal J. Prospective evaluation of the anatomy of the coronary venous system using multidetector row computed tomography. *Int J Cardiol.* 2008; 126:204–208. <https://doi.org/10.1016/j.ijcard.2007.03.128> PMID: 17493696
12. Ma H, Tang Q, Yang Q, Bi X, Li H, Ge L, et al. Contrast-enhanced whole-heart coronary MRA at 3.0T for the evaluation of cardiac venous anatomy. *Int J Cardiovasc Imaging.* 2010; 27:1003–1009. <https://doi.org/10.1007/s10554-010-9757-2> PMID: 21120611
13. Cubuk R, Aydin A, Tasali N, Yilmazer S, Celik L, Dagdeviren B, et al. Non-invasive evaluation of the coronary venous system in patients with chronic systolic heart failure by 64-detector computed tomography. *Acta Radiol.* 2011; 52:372–377. <https://doi.org/10.1258/ar.2011.100241> PMID: 21498314
14. Chen JJ, Lee WJ, Wang YC, Tsai CT, Lai LP, Hwang JJ, et al. Morphologic and topologic characteristics of coronary venous system delineated by noninvasive multidetector computed tomography in chronic systolic heart failure patients. *J Card Fail.* 2007; 13:482–488. <https://doi.org/10.1016/j.cardfail.2007.02.007> PMID: 17675063
15. Jongbloed MR, Lamb HJ, Bax JJ, Schuijff JD, de Roos A, van der Wall EE, et al. Noninvasive visualization of the cardiac venous system using multislice computed tomography. *J Am Coll Cardiol.* 2005; 45:749–753. <https://doi.org/10.1016/j.jacc.2004.11.035> PMID: 15734621

16. Mlynarski R, Mlynarska A, Sosnowski M. Association between changes in coronary artery circulation and cardiac venous retention: a lesson from cardiac computed tomography. *Int J Cardiovasc Imaging*. 2013; 29:885–890. <https://doi.org/10.1007/s10554-012-0139-9> PMID: 23076605
17. De Marco T, Chatterjee K, Rouleau JL, Parmley WW. Abnormal coronary hemodynamics and myocardial energetics in patients with chronic heart failure caused by ischemic heart disease and dilated cardiomyopathy. *Am Heart J*. 1988; 115:809–815. [https://doi.org/10.1016/0002-8703\(88\)90883-6](https://doi.org/10.1016/0002-8703(88)90883-6) PMID: 3354409
18. Nikolaidis LA, Trumble D, Hentosz T, Doverspike A, Huerbin R, Mathier MA, et al. Catecholamines restore myocardial contractility in dilated cardiomyopathy at the expense of increased coronary blood flow and myocardial oxygen consumption (MvO₂ cost of catecholamines in heart failure). *Eur J Heart Fail*. 2004; 6:409–419. <https://doi.org/10.1016/j.ejheart.2003.09.013> PMID: 15182765
19. Mao S, Shinbane JS, Girsky MJ, Child J, Carson S, Oudiz RJ, et al. Coronary venous imaging with electron beam computed tomographic angiography: Three-dimensional mapping and relationship with coronary arteries. *Am Heart J*. 2005; 150:315–322. <https://doi.org/10.1016/j.ahj.2004.09.050> PMID: 16086937
20. Tada H, Kurosaki K, Naito S, Koyama K, Itoi K, Ito S, et al. Three-dimensional visualization of the coronary venous system using multidetector row computed tomography. *Circ J*. 2005; 69:165–170. <https://doi.org/10.1253/circj.69.165> PMID: 15671607
21. Abbara S, Cury RC, Nieman K, Reddy V, Moselewski F, Schmidt S, et al. Noninvasive evaluation of cardiac veins with 16-MDCT angiography. *AJR Am J Roentgenol*. 2005; 185:1001–1006. <https://doi.org/10.2214/AJR.04.1382> PMID: 16177423
22. Mlynarski R, Mlynarska A, Sosnowski M. Anatomical variants of coronary venous system on cardiac computed tomography. *Circ J*. 2011; 75:613–618. <https://doi.org/10.1253/circj.cj-10-0736> PMID: 21242643
23. Genc B, Solak A, Sahin N, Gur S, Kalaycioglu S, Ozturk V, et al. Assessment of the coronary venous system by using cardiac CT. *Diagn Interv Radiol*. 2013; 19:286–293. <https://doi.org/10.5152/dir.2013.012> PMID: 23337097
24. Bax JJ, Abraham T, Barold SS, Breithardt OA, Fung JW, Garrigue S, et al. Cardiac resynchronization therapy: part 1—issues before device implantation. *J Am Coll Cardiol*. 2005; 46:2153–2167. <https://doi.org/10.1016/j.jacc.2005.09.019> PMID: 16360042
25. Boonyasirinant T, Halliburton SS, Schoenhagen P, Lieber ML, Flamm SD. Absence of coronary sinus tributaries in ischemic cardiomyopathy: An insight from multidetector computed tomography cardiac venographic study. *J Cardiovasc Comput Tomogr*. 2016; 10:156–161. <https://doi.org/10.1016/j.jcct.2016.01.015> PMID: 26857422
26. Randhawa A, Saini A, Aggarwal A, Rohit MK, Sahni D. Variance in coronary venous anatomy: a critical determinant in optimal candidate selection for cardiac resynchronization therapy. *Pacing Clin Electrophysiol*. 2013; 36:94–102. <https://doi.org/10.1111/pace.12026> PMID: 23106173
27. Khan FZ, Virdee MS, Gopalan D, Rudd J, Watson T, Fynn SP, et al. Characterization of the suitability of coronary venous anatomy for targeting left ventricular lead placement in patients undergoing cardiac resynchronization therapy. *Europace*. 2009; 11:1491–1495. <https://doi.org/10.1093/europace/eup292> PMID: 19880411
28. Benz DC, Gräni C, Hirt Moch B, Mikulicic F, Vontobel J, Fuchs TA, et al. Minimized radiation and contrast agent exposure for coronary computed tomography angiography: first clinical experience on a latest generation 256-slice scanner. *Acad Radiol*. 2016; 23:1008–1014. <https://doi.org/10.1016/j.acra.2016.03.015> PMID: 27174030